



## Understanding competing mechanisms for glass transition changes in filled elastomers



Charles D. Wood<sup>a</sup>, Amin Ajdari<sup>a</sup>, Craig W. Burkhart<sup>b</sup>, Karl W. Putz<sup>a</sup>,  
L. Catherine Brinson<sup>a, c, \*</sup>

<sup>a</sup> Department of Mechanical Engineering, McCormick School of Engineering and Applied Science, Northwestern University, 2145 Sheridan Road, Evanston, IL 60208, USA

<sup>b</sup> Global Materials Science Division, The Goodyear Tire & Rubber Company, 142 Goodyear Blvd., Akron, OH 44305, USA

<sup>c</sup> Department of Materials Science and Engineering, Northwestern University, 2220 Campus Drive, Evanston, IL 60208-3108, USA

### ARTICLE INFO

#### Article history:

Received 22 October 2015

Received in revised form

15 February 2016

Accepted 18 February 2016

Available online 22 February 2016

#### Keywords:

Nano composites

Interphase

Thermomechanical properties

Finite element analysis (FEA)

Dynamic mechanical thermal analysis

(DMTA)

### ABSTRACT

In polymeric nanocomposites, shifts in the glass transition temperature ( $T_g$ ) that increase monotonically with particle loading have been attributed to the interphase, in ideally dispersed, attractive systems. However, in elastomeric composites a trend has emerged that shows  $T_g$  shifts first towards higher and then towards lower temperatures with increasing filler volume fraction, when measured via mechanical methods (DMA). At high filler loadings (>10 vol%), glass transition temperatures have been recorded below that of the base polymer, even for systems with attractive interactions between polymer and filler. One-dimensional analytical models and three-dimensional finite elements models were used to investigate the source of a mechanically-induced negative  $T_g$  shift in highly filled systems. The results attribute the origin of the shift towards higher temperatures as an effect of the interphase, while the subsequent shift to lower temperatures as an apparent relaxation time shift that arises solely due to the addition of stiff elastic particles. These replicated shifts explain a consistent trend across the literature and provide some considerations for those designing elastomeric composites with high filler loading.

© 2016 Elsevier Ltd. All rights reserved.

## 1. Introduction

One central benefit of filling polymers with nanoparticles is the relatively low volume fractions needed to realize noticeable changes in both thermal and mechanical properties [1–6]. An important material property for viscoelastic materials is the glass transition temperature ( $T_g$ ), which denotes the transition between rubbery and glassy behavior with changing temperature.  $T_g$  shifts that occur in nanocomposites are typically attributed to the presence of ‘interphase’, a region of polymer with altered mobility [7–11] that surrounds fillers in polymeric composites. Due to the vast surface area present in nanomaterials, only low volume fractions are needed to create a percolated interphase network, resulting in sizeable changes in a number of physical property improvements – including modulus and strength [12,13], dielectric

properties [14], conductivity [15] and diffusion constants [16] – in addition to shifts in  $T_g$  [4,5,17], which are interpreted as changes in average polymer mobility due to the creation of interphase. For simplicity, we will consider here only situations of attractive interphases – cases in which the polymer and the nanofiller have positive chemical interactions resulting in reduced mobility of polymer in the interphase region and typically thus result in increases of the  $T_g$  and mechanical properties.

However, for some applications, higher filler concentrations are needed to improve stiffness, wear resistance or fracture properties [18,19]. These high filler concentrations often lead to nanoparticle agglomeration or clustering, which limits the extent of interphase percolation and thus the magnitude in  $T_g$  changes observed for similar systems with better dispersion of nanoparticles [3,5,20,21]. Dynamic mechanical analysis (DMA) is a common experimental method used to characterize mechanical properties and detect changes in glass transition temperatures in polymer composites. From this method, the  $T_g$  is most commonly reported as the location of the peak in the  $\tan(\delta)$  spectra,  $E''/E'$  [22]. This mechanical probing method uses an oscillatory load across a temperature

\* Corresponding author. Department of Mechanical Engineering, McCormick School of Engineering and Applied Science, Northwestern University, 2145 Sheridan Road, Evanston, IL 60208, USA.

E-mail address: [cbrinson@northwestern.edu](mailto:cbrinson@northwestern.edu) (L.C. Brinson).

sweep to determine viscoelastic properties and the  $\tan(\delta)$  curve ( $E''/E'$ ). There are cases in the literature in which  $T_g$  peaks measured by DMA for elastomeric nanocomposites show counterintuitive changes, indicating the complexity and competition between mechanisms that hinder chain mobility and those that increase chain mobility [23]. Additionally, with the use of time-temperature superposition (TTSP) relationships, temperature domain properties can be converted to the frequency domain. Generally,  $\tan(\delta)$  shifts in the temperature domain are inversely proportional to those in the frequency domain.

## 2. Materials and methods

Samples were provided by Goodyear Tire and Rubber Company and used as received. Experimental methods for dynamic mechanical thermal analysis and finite element modeling in this paper have been reported previously [24].

## 3. Results and discussion

In Fig. 1b-c, we present data representative of a carbon black filled elastomer [24]. The glass transition temperature increases slightly at 9 vol% but then decreases thereafter, even below the neat polymer  $T_g$  location. This trend is, as expected, mirrored inversely in the frequency domain, Fig. 1c. If interphase effects increase monotonically with filler volume fractions,  $T_g$  shifts should only progress in one direction (toward higher temperatures and lower frequencies in this case). However, in this case, we observe shifts in both directions as filler loading increases, even though the

components of the composites are identical, and indicate the presence of a complex mechanism that requires more study. Interestingly, variations of this phenomenon shown in Fig. 1d are present in publications that span numerous combinations of elastomer matrices and filler types [23,25–33].

The fact that we observe a lower  $T_g$  at 28 vol% (Fig. 1d) than the neat polymer is particularly interesting and raises some questions. Studied independently, the trends in this particular data set and similar data have been ascribed to changes in matrix properties (degradation, negative interphase effects) caused by processing and to filler aggregation differences with changing volume fraction [27,28,33]. However, the consistency across the literature indicates that there can be a unifying underlying source of the behavior. In this study, we examine these  $T_g$  shifts in elastomeric composites thoroughly and demonstrate clearly the competing effects of the interphase and an important second mechanism due to elastic filler particles.

### 3.1. One-dimensional relaxation shifting

As outlined, negative temperature shifts are pervasive across the literature for elastomeric composites with high vol/wt fractions as measured via DMA. For example, in a publication from Sun et al. [33], they report a positive  $T_g$  shift at lower filler fractions (<10 wt%) that then trends strongly negative thereafter; similar to the data displayed in Fig. 1. Additionally, they show negative DMA results for two filler types at 20 wt%, however, little to no shift when measured via DSC.

In Fig. 2 we plot the DSC and DMA  $T_g$  changes for eight unique

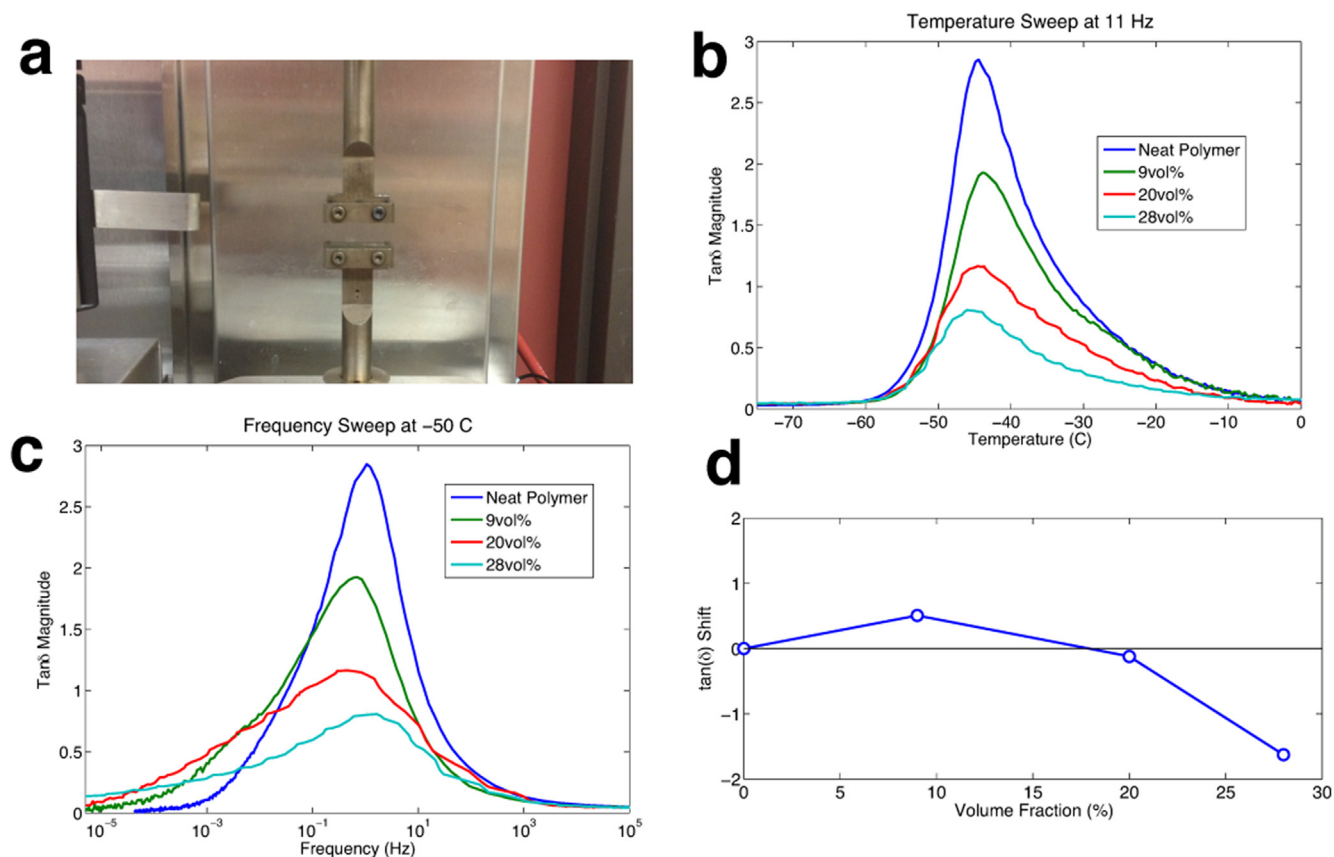


**Fig. 1.** Dynamic Mechanical Analysis (DMA) is a common experimental technique for determining viscoelastic properties of polymer-based materials. Experimental set-up (a). Of particular interest in this study are the  $\tan(\delta)$  spectra represented in the temperature (b) and frequency domains (c); each curve represents one sample and is not averaged. Corresponding glass transition temperature ( $T_g$ ) shifts are plotted to show a shift towards higher temperatures at 9 vol% followed by a shift towards lower temperatures (d) [24].

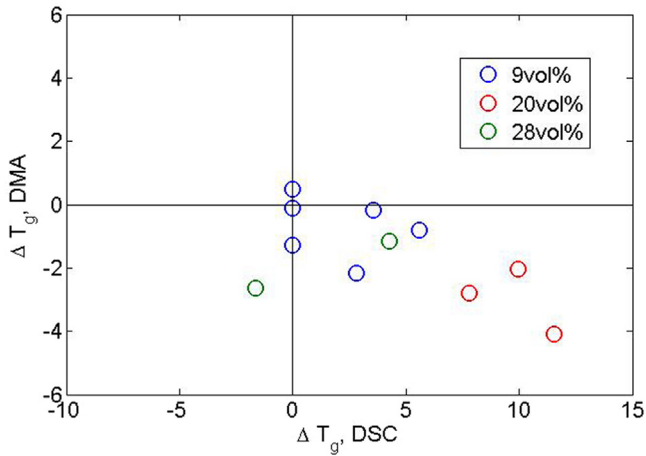


**Fig. 2.** Thermal-based measurements are compared against mechanical measurements of the glass transition shift for eight different rubber-carbon filler combinations. The disagreement between the two measurements highlights some underlying mechanism that influences mechanical measurements.

polymer-filler combinations. In all but one sample, we observe increases in  $T_g$  according to DSC however a decrease according to DMA. The general discord between DSC (+) and DMA (-) is not unique to this dataset and points to a fundamental disconnect between the two measurements at high filler volume fractions. Interphase gradients depend heavily upon the nature of the chemical interactions [34,35] between the polymer and filler and specific for particular systems, and thus would only explain a shift to either higher OR lower temperatures. In these cases, a negative  $T_g$  shift is only observed in DMA data sets and is defined in this paper as a *mechanically-induced negative  $T_g$  shift in highly filled systems*. If the source of this shift is purely mechanical, it would be consistent across the various chemically different systems, and therefore, we should be able to reproduce the trends using various mechanistic models.

For simplicity, we start by analyzing a common one-dimensional model for a time-dependent response, a Kelvin-Voigt Solid. This model contains only three components, two springs and a damper, and importantly, no interphase that shifts the relaxations in the positive direction. The known solution for the system relaxation time,  $\tau_{KV}$ , is expressed as a function of the natural relaxation of the damper, as well as the stiffness of both springs, Eq. (1) [22]. A similar relationship,  $\tau_M$ , also exists for a different

arrangement, Maxwell's model with a series spring (Fig. 3), Eq. (2).

$$\tau_{kv} = \frac{\eta_1}{E_1 + E_2} = \frac{\tau_1 E_1}{E_1 + E_2} \tag{1}$$

$$\tau_m = \frac{\eta_1(E_1 + E_2)}{E_1 E_2} = \frac{\tau_1(E_1 + E_2)}{E_2} \tag{2}$$

With these simple models, we can begin to model a composite on a rudimentary level. We do that by letting the single spring ( $E_2$ ) represent our hard particle, and the Kelvin element (spring and damper in parallel,  $E_1$  and  $\eta_1$ ) the polymer. The relaxation time of the damper in the polymer unit is defined as  $\tau_1$ , which is the damping coefficient divided by the spring stiffness ( $\eta_1/E_1$ ). Eq. (1) defines the relaxation time of the total system ( $\tau_{KV}$ ) as a function of the spring and damper constants according to the Kelvin-Voigt configuration. This relationship demonstrates that although there is a single relaxation time defined for the damper, the system relaxation depends upon the stiffness ratio of the two springs. We can then introduce further complexity by introducing weighting factors to account for phase volume fractions to customize the system. In Eq. (3) and Eq. (4), we define the relaxation time of the composite ( $\tau_{composite}$ ) as a function of the polymer stiffness ( $E_1$ ), polymer relaxation time ( $\tau_1$ ), particle stiffness ( $E_2$ ) and particle volume fraction ( $V_f$ ).

$$\tau_{composite, KV} = \frac{\tau_1(1 - V_f)E_1}{(1 - V_f)E_1 + (V_f)E_2} \tag{3}$$

$$\tau_{composite, M} = \frac{\tau_1((1 - V_f)E_1 + (V_f)E_2)}{(V_f)E_2} \tag{4}$$

By inspection of Eq. (3), we can deduce that the composite relaxation time will gradually decrease with increasing volume fraction of elastic filler as long as the particle spring is stiffer than the polymer spring ( $E_1 < E_2$ ) and the polymer relaxation time does not change. Additionally, as the stiffness of the polymer spring decreases, the shift becomes larger. The Maxwell model, Eq. (4), does not exhibit this type of response mainly because it has a simple fluid-like architecture. This basic shifting concept has been discussed with respect to a one dimensional model [23], but has not been studied in depth with more complex mechanical models. Expanding from this simple model, we can represent the elastomer with 27 Maxwell models (or a Prony series), as shown in Fig. 4a, to

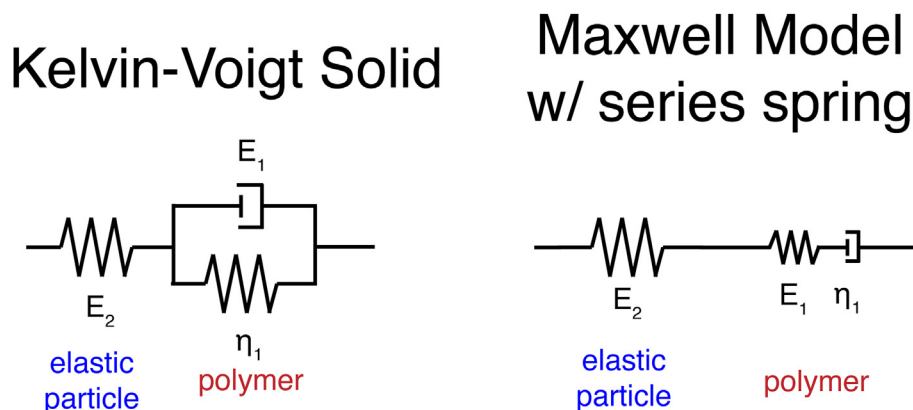


**Fig. 3.** Two different simple one-dimensional models are created to study the effects of fillers on the composite relaxation time; a Kelvin-Voigt Solid and a Maxwell model in series with a spring. These two models represent the particle as a spring and the polymer as a combination of a spring and a damper, giving it simple viscoelastic behavior.

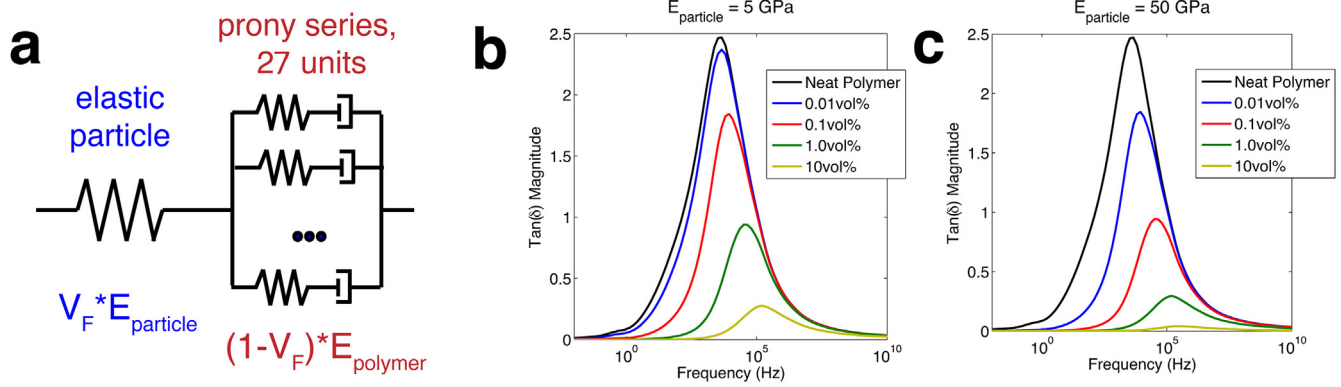


**Fig. 4.** A one-dimensional model is constructed that models an elastomeric composite with increasing volume fraction using an elastic spring in series with a 27 unit prony series (a). When the particles are introduced ( $>0$  vol%), the  $\tan(\delta)$  peaks shift immediately to higher frequencies and reduce in magnitude. The magnitude of this shift and the drop in the maximum of  $\tan(\delta)$  is tied to the stiffness of the particle phase, 5 GPa (b) and 50 GPa (c). The shifting with increasing particle volume fraction is consistently towards increasing 'relaxation frequency' and thus decreasing relaxation time.

represent the spectra of relaxation times. Transforming the elastic response to the frequency domain through a Fourier transform and increasing the volume fraction of the filler, the  $\tan(\delta)$  peak, or mean relaxation frequency, simultaneously drops and shifts towards higher frequencies immediately, shown in Fig. 4b, corresponding to increasing relaxation times.

The coupling of a stiff elastic spring to the polymer shifts the  $\tan(\delta)$  peak towards higher frequencies, analogous to negative temperature shifts. The magnitude of this shift is tied to the stiffness of the particle phase, as evident in Fig. 4b–c. However, in this simplified case, the shift happens very early, well before 1 vol%. The results from this one-dimensional model replicate a limit case of the effect we observed in the experimental DMA data. Since the polymer properties in these simulations remain constant, the perceived shift in mean relaxation times are due to the addition of stiffer elastic particles, which alter the effective relaxation time of the composite system. As demonstrated in the simplified model, this effect can appear in any polymeric system as long as there is a suitably large stiffness difference between the filler and base polymer system.

While this one-dimensional model is valuable in clearly demonstrating the origin of this additional shifting mechanism in elastomer composites, the geometry is, naturally, oversimplified. In physical composites, the particles are dispersed typically randomly in three dimensions. Therefore below we examine more complex mechanical simulations.

### 3.2. Three-dimensional models of random arrays

Three-dimensional finite element models ( $20 \times 20 \times 20$ ) with periodic boundary conditions were created using Abaqus CAE to model a realistic response of a virtual elastomeric composite. These models allow for representations of particle dispersions, which should translate to the realized mechanical properties. Consistent with the one-dimensional model, these models contain only two phases: a prony series characterizing an elastomer and an elastic stiff particle ( $E_p = 50$  GPa). The stiff particles were randomly dispersed to represent a mean or average response as a function of volume fraction. The dispersions created contain a no-bias, random, uniform distribution, and attempt to represent a general increase in particle concentration, with no additional complexities such as change in particle clustering propensity. The output from the model demonstrates that particles reinforce the elastomer and increase the overall stiffness, resulting in both storage ( $E'$ ) and loss ( $E''$ ) moduli changes as shown in Fig. 5a; however, the introduction

of particles affects  $E'$  and  $E''$  in different ways. Most notable is the dramatic changes in  $E'$  in the rubber-glass transition region. The transition zone exhibits an effective shortening which is caused by an unbalanced reinforcement of the rubbery ( $E_{inf}$ , low frequency) and glassy ( $E_0$ , high frequency) moduli. As can be expected, stiff particles are more efficient at reinforcing low modulus materials and therefore reduce the magnitude of the glassy-rubbery transition for  $E'$ . The loss modulus,  $E''$  shifts up and broadens slightly. These simultaneous changes in  $E'$  and  $E''$  correspond to a significant and progressive shift in the  $\tan(\delta)$  as a function of particle loading, shown in Fig. 5b in the frequency domain and in Fig. 5d in the temperature domain. The  $\tan(\delta)$  in the temperature domain, Fig. 5d–e, is calculated directly by transformation (see Supplementary Information).  $\tan(\delta)$  is a fundamental measure of material damping and the significant reductions in  $\tan(\delta)$  are due to the incorporation of perfectly elastic particles (no damping) which replace a given volume of polymeric (damping) material in the composites.

These 3D composite simulations confirm the trends illustrated with the simple 1D analytical model: addition of elastic particles leads to decreases and shifts in  $\tan(\delta)$ . Note that the three-dimensional dispersion of particles in the elastomer matrix result in a realistic gradual decay of the spectra magnitude with volume fraction additions, as opposed to the sharp changes observed with only one degree of freedom. Likewise, the shift of the peak is gradual and grows as the volume fraction increases, shown in Fig. 5c–e where the position of the  $\tan(\delta)$  peak as a function of volume fraction is calculated.

Since the particle dispersions were created by random generation, additional models were independently created through the same procedure to determine the variation in the shifting trends for random dispersions, Fig. 6. The three model outputs have only minor variations and show a strong and consistent shifting trend after 5 vol%. The small variations in the shifting position are due to varying amounts of agglomeration and particle-to-particle distances in each randomly generated model. A power-law fit defines the overall trend of the combined three data sets with a strong R-squared correlation. Interestingly, the shifting trend begins well before particle-to-particle percolation, which traditionally happens at high filler fractions, around 20–30% for spheres [36].

To translate the shifting mechanisms observed to the impact on realistic elastomeric composites, we perform a simulation of a representative microstructure of a filled elastomer. In this simulation the shifting of  $\tan(\delta)$  to high freq/low T due to the stiff particles and reduced dissipation is automatically included by virtue of the

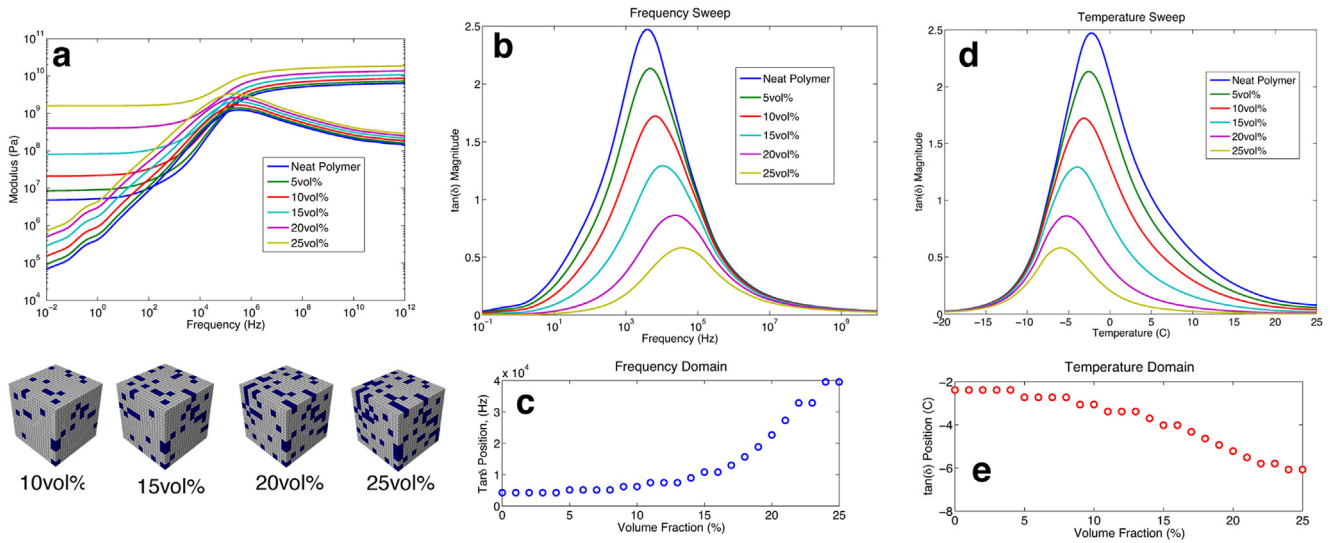


**Fig. 5.** A three-dimensional finite element model was constructed to represent a realistic  $\tan(\delta)$  behavior as particles concentration increases. The results – storage/loss modulus in (a) and  $\tan(\delta)$  in (b) – show a progressive shifting mechanism that both reduces  $\tan(\delta)$  magnitude and shifts the peak to higher frequencies (c). The  $\tan(\delta)$  shift to higher frequencies corresponds to a shift to lower temperatures (d, e).

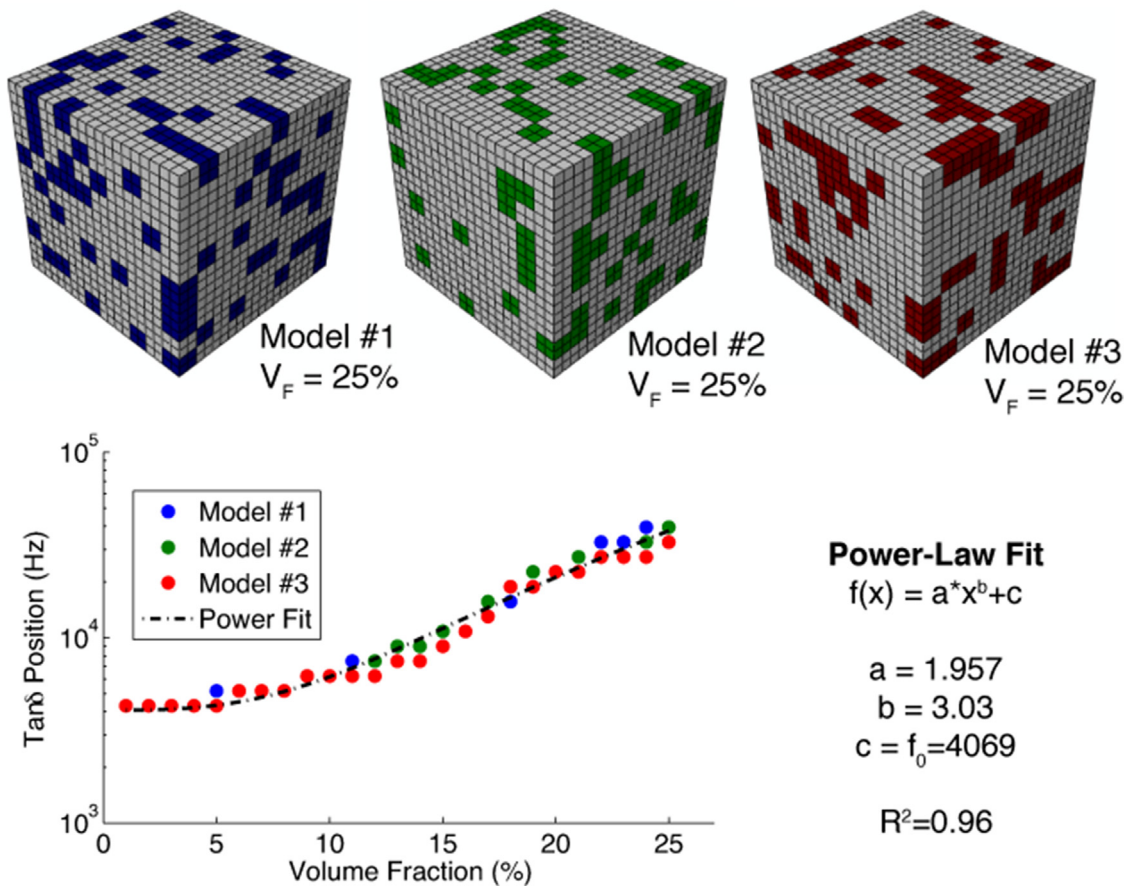


**Fig. 6.** Three independent and randomly constructed finite element models were compared at each volume fraction to define the overall  $\tan(\delta)$  shifting mechanism. The results show little variation between the models as well as a power-law behavior that grows considerably after 5 vol%.

morphology of the simulated geometry. We also include the interphase polymer domains that exist near the particles with enhanced properties [37,38] to account for shifting in  $\tan(\delta)$  due to changes in polymer mobility near particles. To account for the

gradient of properties in the interphase zone, we use two layers of interphase with properties chosen to be related to the bulk matrix material by  $T_g$  shifts; the first with properties shifted two decades from that of the bulk matrix material (to lower frequency) and the

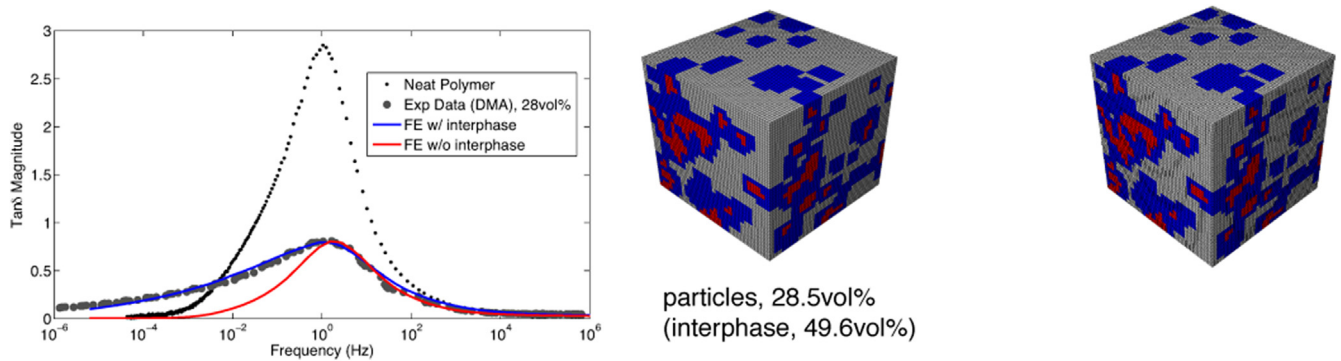


**Fig. 7.** Finite element models ( $60 \times 60 \times 60$ ) with representative microstructures and interphase gradients match experimental results at high filler concentrations, even when  $\tan(\delta)$  appears to shift to higher frequencies, or lower temperatures [24]. We observe that the peak position, at this high filler loading, is nearly the same with or without interphase, therefore controlled by the presence of the stiff phase.

second layer shifted one decade from the neat polymer. These assumptions thus simulate a positive  $T_g$  shift in the interphase regime corresponding to attractive interactions between the polymer network and the filler particles [7]. To create a realistic morphology, instead of random particle placements, the microstructure here is created based upon a reconstruction using SEM images of a filled rubber [24,39]. The care taken to recreate a realistic dispersion is important, as it will more closely represent the amount of filler interface available for interphase creation. Improvements in dispersion are typically associated with an increase in the amount of interphase polymer and thus its impact on shifting of the  $\tan \delta$  peak of the composite, as has been discussed both from experimental data and in computational studies [3,5,20,21].

With three phases (polymer, particle, interphase), FE models compare nicely to experimental data, even for the highly filled system at 28 vol% as in Fig. 7. With interphase polymer gradients that account for nearly 50% of the model, the model matches the right position and shape of the  $\tan(\delta)$  spectra. Since the interphase polymer properties are shifted to lower frequencies (higher temperatures) than the bulk matrix material, there is a broadening of the composite peak toward lower frequencies, however the overall shift of the peak is towards higher frequencies. It is notable that the predictions without interphase demonstrate only the mechanically-induced shifting to high frequency and that the result has nearly the same peak location as the results including interphase effects. This finding indicates that in the highly filled system, the mechanical reduced damping effect dominates the interphase polymer effect, even where significant interphase volume fractions are included. The results provide understanding that composite systems with positive interphase effects can still demonstrate an effective lower  $T_g$  than the base polymer at high volume fractions. This mechanical shifting mechanism will be observed in DMA tests which probe for this property in thermo-mechanical loading space. However  $T_g$  values measured by heat flow in DSC are not mechanically loaded and the reduced damping effect from the elasticity of the fillers is removed.

#### 4. Conclusions

The results from the two-phase models reveal the source of a mechanically induced negative  $T_g$  shift, or positive frequency shift, in highly filled systems. We demonstrate that the apparent mean relaxation time of the composite shifts to shorter times without any alterations to the polymer or chemical considerations. This shift depends upon two things: the volume fraction of the stiff phase (particles) and the stiffness of the matrix phase in the transition

region. A simple one-dimensional model reveals that the shifting is more intense when the particles are much stiffer ( $> \times 10$ ) than the matrix. This stiffness mismatch also creates an asymmetric shift to the  $\tan(\delta)$  spectra, where  $E'$  transitions from rubbery to glassy. We also demonstrate that three-dimensional FE models capture this mechanical relaxation shift with regularity, and can be integrated with interphase gradients to match the correct position of the  $\tan(\delta)$  curve from an experimental sample.

Additionally, these results have interesting implications in terms of material design. First, the particle-induced shifting mechanism due to the elastic filler can explain negative composite  $T_g$  shifts without recourse to assumptions of degradation in matrix properties or changing agglomeration with volume fraction. Three-dimensional FE models demonstrate that at high filler concentrations  $\tan(\delta)$  peaks can appear to shift to higher frequencies even though interphase effects are positive. The shift also explains why thermal-based methods of defining  $T_g$  (DSC) would disagree with mechanically measured DMA results (eg Ref. [33]). It is noted that DMA measurements for  $T_g$  are widely used and for many applications where the polymer composite is being mechanically loaded under varying temperatures, this may be the most relevant measure.

Secondly, the shifting mechanism implies that a maximum  $T_g$  exists at lower filler concentrations for a given polymer/filler pair. The hypothesized inflection point is a consequence of early ( $< 5$  vol %) shifting due to attractive interphase and the delayed elastic particle-based shift. This maximal point exists where the particle-induced relaxation time shift begins to overtake positive influences of interphase regimes. Because the two effects occur simultaneously, it allows the peaks to shift in both directions while keeping all other considerations constant. However, if interphase effects are not strongly positive, it is possible peaks will simply shift towards lower temperatures monotonically. The magnitude of perceived  $T_g$  shifts and their location (vol%) depend upon several factors, most including the amount of interphase present and associated factors, such as filler morphology and dispersion quality.

#### Acknowledgements

Support for this project was provided by Goodyear Tire and Rubber Company (Akron, OH) (4507401163). Differential Scanning Calorimetry (DSC) data was collected at the Integrated Molecular Science and Education Center (IMSERC) at Northwestern University. The authors would also like to thank Charlotte Stern and Stephen Marrou for assistance with collecting DSC data.

## Appendix A. Supplementary data

Supplementary data related to this article can be found at <http://dx.doi.org/10.1016/j.compscitech.2016.02.027>.

## References

- [1] M.J. Palmeri, K.W. Putz, T. Ramanathan, L.C. Brinson, Multi-scale reinforcement of CFRPs using carbon nanofibers, *Compos. Sci. Technol.* 71 (2) (2010) 79–86.
- [2] K.W. Putz, M.J. Palmeri, R.B. Cohn, R. Andrews, L.C. Brinson, Effect of cross-link density on interphase creation in polymer nanocomposites, *Macromolecules* 41 (18) (2008) 6752–6756.
- [3] R. Qiao, H. Deng, K.W. Putz, L.C. Brinson, Effect of particle agglomeration and interphase on the glass transition temperature of polymer nanocomposites, *J. Polym. Sci. Pol. Phys.* 49 (10) (2011) 740–748.
- [4] T. Ramanathan, S. Stankovich, D.A. Dikin, H. Liu, H. Shen, S.T. Nguyen, et al., Graphitic nanofillers in PMMA nanocomposites—An investigation of particle size and dispersion and their influence on nanocomposite properties, *J. Polym. Sci. Part B Polym. Phys.* 45 (15) (2007) 2097–2112.
- [5] T. Ramanathan, A.A. Abdala, S. Stankovich, D.A. Dikin, M. Herrera Alonso, R.D. Piner, et al., Functionalized graphene sheets for polymer nanocomposites, *Nat. Nano* 3 (6) (2008) 327–331.
- [6] H.B. Yang, F.Z. Li, T.W. Chan, L. Liu, L.Q. Zhang, A simulation study on the effect of spring-shaped fillers on the viscoelasticity of rubber nanocomposite, *Compos. Part B Eng.* 74 (2015) 171–177.
- [7] C.J. Ellison, J.M. Torkelson, The distribution of glass-transition temperatures in nanoscopically confined glass formers, *Nat. Mater.* 2 (10) (2003) 695–700.
- [8] P. Rittigstein, R.D. Priestley, L.J. Broadbelt, J.M. Torkelson, Model polymer nanocomposites provide an understanding of confinement effects in real nanocomposites, *Nat. Mater.* 6 (4) (2007) 278–282.
- [9] M.K. Mundra, C.J. Ellison, R.E. Behling, J.M. Torkelson, Confinement, composition, and spin-coating effects on the glass transition and stress relaxation of thin films of polystyrene and styrene-containing random copolymers: sensing by intrinsic fluorescence, *Polymer* 47 (22) (2006) 7747–7759.
- [10] S. Watcharotone, C.D. Wood, R. Friedrich, X.Q. Chen, R. Qiao, K. Putz, et al., Interfacial and substrate effects on local elastic properties of polymers using coupled experiments and modeling of nanoindentation, *Adv. Eng. Mater.* 13 (5) (2011) 400–404.
- [11] X. Cheng, K.W. Putz, C.D. Wood, L.C. Brinson, Characterization of local elastic modulus in confined polymer films via AFM indentation, *Macromol. Rapid Commun.* 36 (4) (2015) 391–397.
- [12] A. Eitan, F.T. Fisher, R. Andrews, L.C. Brinson, L.S. Schadler, Reinforcement mechanisms in MWCNT-filled polycarbonate, *Compos. Sci. Technol.* 66 (9) (2006) 1162–1173.
- [13] H. Liu, L.C. Brinson, Reinforcing efficiency of nanoparticles: a simple comparison for polymer nanocomposites, *Compos. Sci. Technol.* 68 (6) (2008) 1502–1512.
- [14] Y. Shen, Y. Lin, M. Li, C.W. Nan, High dielectric performance of polymer composite films induced by a percolating interparticle barrier layer, *Adv. Mater.* 19 (10) (2007) 1418–1422.
- [15] S. Stankovich, D.A. Dikin, G.H.B. Dommett, K.M. Kohlhaas, E.J. Zimney, E.A. Stach, et al., Graphene-based composite materials, *Nature* 442 (7100) (2006) 282–286.
- [16] C. Wei, D. Srivastava, K. Cho, Thermal expansion and diffusion coefficients of carbon nanotube-polymer composites, *Nano Lett.* 2 (6) (2002) 647–650.
- [17] F.T. Fisher, A. Eitan, R. Andrews, L.S. Schadler, L.C. Brinson, Spectral response and effective viscoelastic properties of MWNT-reinforced polycarbonate, *Adv. Compos. Lett.* 13 (2) (2004) 105–111.
- [18] K. Friedrich, Z. Zhang, A.K. Schlarb, Effects of various fillers on the sliding wear of polymer composites, *Compos. Sci. Technol.* 65 (15–16) (2005) 2329–2343.
- [19] W.G. Sawyer, K.D. Freudenberg, P. Bhimaraj, L.S. Schadler, A study on the friction and wear behavior of PTFE filled with alumina nanoparticles, *Wear* 254 (5–6) (2003) 573–580.
- [20] J. Cho, I.M. Daniel, Reinforcement of carbon/epoxy composites with multi-wall carbon nanotubes and dispersion enhancing block copolymers, *Scr. Mater.* 58 (7) (2008) 533–536.
- [21] R.K. Duncan, R. Qiao, J.B. Bult, D. Burris, L.C. Brinson, L.S. Schadler, Viscoelastic behavior of nanotube-filled polycarbonate: effect of aspect ratio and interface chemistry, *Int. J. Smart Nano Mater.* 1 (1) (2010) 53–68.
- [22] H.F. Brinson, L.C. Brinson, *Polymer Engineering Science and Viscoelasticity: an Introduction*, Springer, New York, 2008.
- [23] V. Arrighi, I.J. McEwen, H. Qian, M.B.S. Prieto, The glass transition and interfacial layer in styrene-butadiene rubber containing silica nanofiller, *Polymer* 44 (20) (2003) 6259–6266.
- [24] H. Deng, Y. Liu, D.H. Gai, D.A. Dikin, K.W. Putz, W. Chen, et al., Utilizing real and statistically reconstructed microstructures for the viscoelastic modeling of polymer nanocomposites, *Compos. Sci. Technol.* 72 (14) (2012) 1725–1732.
- [25] E. Donth, M. Beiner, S. Reissig, J. Korus, F. Garwe, S. Vieweg, et al., Fine structure of the main transition in amorphous polymers: entanglement spacing and characteristic length of the glass transition. Discussion of examples, *Macromolecules* 29 (20) (1996) 6589–6600.
- [26] J. Frohlich, R. Thomann, R. Mulhaupt, Toughened epoxy hybrid nanocomposites containing both an organophilic layered silicate filler and a compatibilized liquid rubber, *Macromolecules* 36 (19) (2003) 7205–7211.
- [27] M. Jacob, B. Francis, S. Thomas, K.T. Varughese, Dynamical mechanical analysis of sisal/oil palm hybrid fiber-reinforced natural rubber composites, *Polym. Compos.* 27 (6) (2006) 671–680.
- [28] M.A. Lopez-Manchado, J. Biagiotti, L. Valentini, J.M. Kenny, Dynamic mechanical and raman spectroscopy studies on interaction between single-walled carbon nanotubes and natural rubber, *J. Appl. Polym. Sci.* 92 (5) (2004) 3394–3400.
- [29] M.A.L. Manchado, L. Valentini, J. Biagiotti, J.M. Kenny, Thermal and mechanical properties of single-walled carbon nano tubes-polypropylene composites prepared by melt processing, *Carbon* 43 (7) (2005) 1499–1505.
- [30] J.K. Mishra, I. Kim, C.S. Ha, New millable polyurethane/organoclay nanocomposite: preparation, characterization and properties, *Macromol. Rapid Commun.* 24 (11) (2003) 671–675.
- [31] P. Potschke, M. Abdel-Goad, I. Alig, S. Dudkin, D. Lellinger, Rheological and dielectrical characterization of melt mixed polycarbonate-multiwalled carbon nanotube composites, *Polymer* 45 (26) (2004) 8863–8870.
- [32] G. Tsagaropoulos, A. Eisenberg, Direct observation of 2 glass transitions in silica-filled polymers - implications for the morphology of random ionomers, *Macromolecules* 28 (1) (1995) 396–398.
- [33] Y.Y. Sun, Z.Q. Zhang, K.S. Moon, C.P. Wong, Glass transition and relaxation behavior of epoxy nanocomposites, *J. Polym. Sci. Pol. Phys.* 42 (21) (2004) 3849–3858.
- [34] B. Natarajan, Y. Li, H. Deng, L.C. Brinson, L.S. Schadler, Effect of interfacial energetics on dispersion and glass transition temperature in polymer nanocomposites, *Macromolecules* 46 (7) (2013) 2833–2841.
- [35] L.M. Hamming, R. Qiao, P.B. Messersmith, L. Catherine Brinson, Effects of dispersion and interfacial modification on the macroscale properties of TiO<sub>2</sub> polymer-matrix nanocomposites, *Compos. Sci. Technol.* 69 (11–12) (2009) 1880–1886.
- [36] Y.-B. Yi, A.M. Sastry, Analytical approximation of the percolation threshold for overlapping ellipsoids of revolution, *Proc. R. Soc. Lond. Ser. A Math. Phys. Eng. Sci.* 460 (2048) (2004) 2353–2380.
- [37] C.P. Tsui, C.Y. Tang, T.C. Lee, Finite element analysis of polymer composites filled by interphase coated particles, *J. Mater. Process. Technol.* 117 (1–2) (2001) 105–110.
- [38] F.T. Fisher, L.C. Brinson, Viscoelastic interphases in polymer-matrix composites: theoretical models and finite-element analysis, *Compos. Sci. Technol.* 61 (5) (2001) 731–748.
- [39] H. Xu, M.S. Greene, H. Deng, D. Dikin, C. Brinson, W. Kam Liu, et al., Stochastic reassembly strategy for managing information complexity in heterogeneous materials analysis and design, *J. Mech. Des.* 135 (10) (2013), 101010–101010.